


ITC 4/51 Information Technology and Control Vol. 51 / No. 4 / 2022 pp. 692-703 DOI 10.5755/j01.itc.51.4.31323	Lion Based Butterfly Optimization with Improved YOLO-v4 for Heart Disease Prediction Using IoMT	
	Received 2022/05/02	Accepted after revision 2022/06/17
	 http://dx.doi.org/10.5755/j01.itc.51.4.31323	

HOW TO CITE: Alamelu, V., Thilagamani, S. (2022). Lion Based Butterfly Optimization with Improved YOLO-v4 for Heart Disease Prediction Using IoMT. *Information Technology and Control*, 51(4), 692-703. <http://dx.doi.org/10.5755/j01.itc.51.4.31323>

Lion Based Butterfly Optimization with Improved YOLO-v4 for Heart Disease Prediction Using IoMT

V. Alamelu, S. Thilagamani

Department of Computer Science and Engineering, M. Kumarasamy College of Engineering, Karur, 639113, India; e-mail: valamelu12@outlook.com

Corresponding author: valamelu12@outlook.com

The Internet of Medical Things (IoMT) has subsequently been used in healthcare services to gather sensor data for the prediction and diagnosis of cardiac disease. Recently image processing techniques require a clear focused solution to predict diseases. The primary goal of the proposed method is to use health information and medical pictures for classifying the data and forecasting cardiac disease. It consists of two phases for categorizing the data and prediction. If the previous phase's results are practical heart problems, then there is no need for phase 2 to predict. The first phase categorized data collected from healthcare sensors attached to the patient's body. The second stage evaluated the echocardiography images for the prediction of heart disease. A Hybrid Lion-based Butterfly Optimization Algorithm (L-BOA) is used for classifying the sensor data. In the existing method, Hybrid Faster R-CNN with SE-Rest-Net-101 is used for classification. Faster R-CNN uses areas to locate the item in the picture. The proposed method uses Improved YOLO-v4. It increases the semantic knowledge of little things. An Improved YOLO-v4 with CSPDarkNet53 is used for feature extraction and classifying the echo-cardiogram pictures. Both categorization approaches were used, and the results were integrated and confirmed in the ability to forecast heart disease. The LBO-YOLO-v4 process detected regular sensor data with 97.25% accuracy and irregular sensor data with 98.87% accuracy. The proposed improved YOLO-v4 with the CSPDarkNet53 method gives better classification among echo-cardiogram pictures.

KEYWORDS: YOLO-v4, CSPDarkNet53, heart disease, Internet of Medical Things (IoMT), Butterfly Optimization Algorithm, classification, prediction, sensor data, diagnosis.

1. Introduction

Smart healthcare is competent healthcare for medical systems that use intelligent devices, the Internet of Things, and the Internet Service to access medical data directly and integrate services, persons, and organizations. Doctors, workers, institutions, and scientific institutions are just a few people involved in patient monitoring. Diseases identification and monitoring, decision-making, health administration, and clinical science are part of this dynamic setting. Automatic systems, including the Internet of Things (IoT), artificial intelligence (AI), Big Data, cloud networking, and 5G, as well as enhanced biotech, are all part of intelligent medicine [16].

The provision of medicine is a basic societal obligation [4]. In the medical industry, big data covers a wide range of topics. Any data explicitly or implicitly relevant to health care falls into this category: biomedical data, global health information, health outcomes, medical insurance information, and health services data. Environmental parameters, administration, clinical science data, and community health improvement data are among the most common groups. Various strategies are designed in this sector based on machine learning techniques commonly used to tackle issues, including prediction, extraction of features, and categorization.

The author introduced the AlexNet convolutional neural network model, which would be regarded as a firm grounding for creating an item testing method based on deep learning in 2012 [30]. Deep learning-based object detection methods are now classified into two types. One is the Two-Stage method, built on R-CNN [27, 3] and TridenNet [5], among other algorithms. The next is the SSD [12, 8, 7] and YOLO-based One-Stage method, which has excellent actual improvement in multi-scale object recognition.

The primary goal of this research is to construct a design for predicting cardiovascular problems. Earlier studies relied on sensor-based data (healthcare signals) or imaging techniques for classification and prediction. Rather than employing sensor and picture data independently in the suggested method, sensors and picture information are integrated as two phases of input. Sensor information can be used for forecasting and categorization during the first phase. At the same time, the first stage's outcome is not suitable,

depending on the severity of the sickness or the produced outputs. The second phase would be employed to classify and predict disease using medical image information accurately. Precision estimations can be developed to meet the needs between both patients and physicians by using this categorization technique. The main contribution of the proposed method LBO-YOLO-v4 is given below:

- The first phase includes classifying sensor data collected by medical sensors attached to the patient's body. The classification of echocardiography pictures follows next in the second phase.
- This work addresses the issue of training time by incorporating the upgraded CSPDark-Net53 into the core to achieve rapid modeling convergence and reduce development time costs.
- A Lion-based Butterfly Optimization Algorithm (L-BOA) is used for classifying the sensor data.
- Improved YOLO-v4 with CSPDarkNet53 is used for feature extraction and classifying the echocardiogram pictures.

The remaining sections of this paper are structured as follows: Section 2 discusses the related research works, Section 3 describes the Lion-based Butterfly Optimization Algorithm (L-BOA), Improved YOLO-v4 with CSPDarkNet53, Section 4 presents the methods used to adopt the proposed model, Section 5 discusses the experimented results and Section 6 concludes the proposed system with future work.

2. Related Works

The author [6] employed a modified deep convolutional neural network (MDCNN) to forecast cardiac illness. A wearable and an ECG gadget were used to monitor a patient's blood pressure and ECG in that study. The MDCNN was utilized to categorize the sensing information recorded as healthy or unhealthy. The efficiency of these models may have been enhanced by using a feature selection technique for greater benefits.

A smart healthcare model based on autoencoders for heart disease detection was suggested in [20]. Physio-

bank-PhysioNet with PASCAL B-training AEN's diagnostics system was built using training heart sound datasets. In [22] employed a learning-aided enhanced deep convolutional neural network (EDCNN) to improve cardiovascular disease prognostics. The framework, which combines an MLP concept with regularization learning methods, was created with deep architecture in consideration. As just an outcome, the decrease in variables had an effect on the results of the classifier in terms of correctness and time consumption.

The author [17] employed superior classifiers called optimum deep learning to categorize cancer, brain scans, and Alzheimer's illness. By using a deep learning approach that included pretreatment, feature selection, and categorization, an optimized feature range of choice medical classification technique was achieved. To increase the classifier's efficiency, the opposition-based crow search (OCS) technique was used. The OCS method selected the optimal qualities for research from pre-processed photos.

In [1], a convolutional neural network (CNN) was utilized to diagnose cardio-vascular illness in patients. The suggested methodology was first centered on spatial representing data with CNN for the prediction of heart disease. To improve performance, extraction of features and feature selection techniques could be used. A mixed fuzzy-based decision tree approach for earlier diagnosis of heart illness was suggested in [26] employing a continuous and distant patient surveillance system.

The collection of RGB color data has been employed by some researchers in conducting face mask recognition [9]. Moreover, because the paper does not really address the issue of non-standard mask-wearing, the system's flexibility has to be enhanced. The researchers in [23] achieved face mask identification using YOLO-v2 and ResNet50, with DarkNet-19 as the backbone network. According to the authors of [10], the mixture of ResNet50 and SVM can recognize face masks with an accuracy of up to 99.64 percent. The method, on the other hand, has high computational complexity.

Table 1

Characteristics and Methodologies used for Disease Prediction

Author	Methodologies Used	Characteristics
Xiao et al. [28]	MRLDC	It detects diseases more quickly. The importance of investigating implicit links is considerable.
Mohan et al. [18]	HRFLM	In terms of effectiveness, the performance level has improved. Disease forecasting has great potential.
Vasquez-Morales Yang et al. [25]	CBR	It is capable of accurately predicting the risk of CKD. The accuracy of the prediction and the rate with which it converges has both been improved.
Yang et al. [29]	EPDP	Depending on the communication and computation operating costs, it is more effective. This method works well in real-time situations.
Hag et al. [2]	SVM	The estimated time is cut in half thanks to feature selection. The general predictive performance of categorization has increased.
Sierra-Sosa et al. [24]	Traditional Machine Learning	The patient information is quickly evaluated, and predictive performance is increased. Flexibility is possible for large data sets.
Karim et al. [11]	Deep-Sparse Autoencoder structure	During training, SAE eliminates aspects that are not needed. ESD offers quick extraction of features and sustained success.
Liu et al. [13]	WOA	It's simple to use. The calculation cost is really minimal.

3. Proposed Methodology

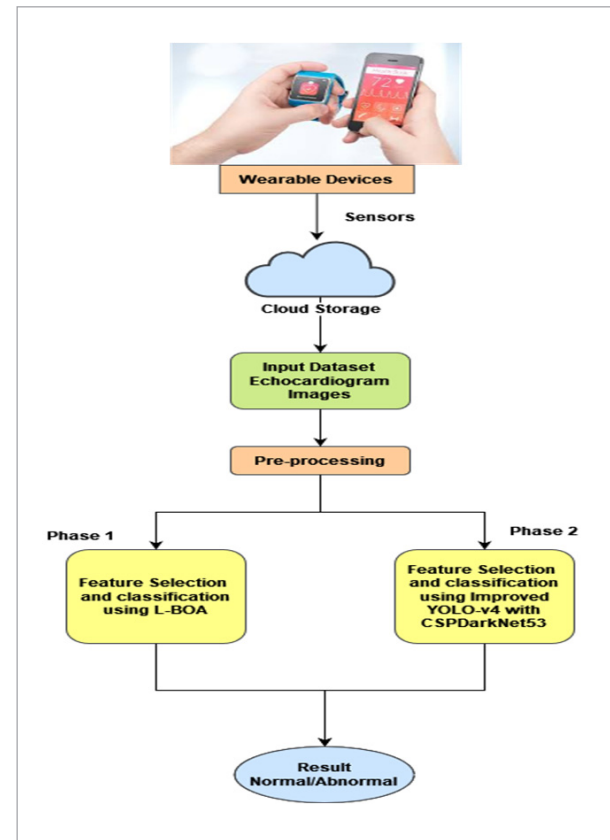
Artificial intelligence and machine learning methods are used in the suggested way for health information prediction and classification. The proposed study relies heavily on sensors (wearables) and databases. There are two phases to the recommended method. Healthcare sensors placed on a person's body produce sensor information in the first phase. This would be followed by categorizing echocardiography pictures in the second phase. Sensor information was recorded and sampled in this investigation, with ECG sensor data at 100 Hz. Data was supplied through Bluetooth to the device and saved as binary and comma-separated value (.csv) formats. The image analysis testing was performed using tailored echocardiogram imaging data collected confidentially under the observation of a physician. Those documents were saved in a cloud-based database. Sensor methods are categorized using the Hybrid Lion-based Butterfly Optimization Algorithm (L-BOA) to classify the sensor data. Improved YOLO-v4 with CSPDarkNet53 is used for feature extraction and organizing the echocardiogram pictures.

Medical information was analyzed using ECG, pulse oximeter, temperatures, and blood pressure sensors in the type of wearables. By placing such devices on the human body, they were capable of recording ECG data, heart rate, blood pressure, and even body temperature. This study was carried out in two phases, every one with its unique set of difficulties. The results of the two phases were found to be accurate in heart disease prediction. From the results of phase 1, users would be able to measure the effects of the disease [21, 14, 15] by measuring ECG, heart rate, and blood pressure. A physician will assess the initial phase outcomes and inform patients of any diagnostic tests needed in phase 2. The information can be analyzed mainly by the physician and the users from afar. Users have to go to the hospital for healthcare assistance in case of emergencies.

The suggested methodology is depicted in Figure 1, and it works as follows: To begin, medical data is measured using sensors (ECG, BP, and pulse oximeter) attached to the patient's body. The information taken by patients' sensors is significant to cardiovascular disease. The path of electric signals when they flow

Figure 1

The architecture of Proposed LBO-YOLO-v4



through the cardiac muscle is detected by the ECG sensors. A heart rate from outside ranges from 60 to 100 beats per minute is considered abnormal.

3.1. Input Dataset

The initial phase is collecting the input data from the cloud storage. Herewith the help of the oximeter sensor the echocardiogram images were collected and stored in the cloud. These data were stored in .csv format. This data is given as input for heart disease prediction.

3.2. Pre-processing

Pre-processing is the next phase in the classification process, it helps to identify the elimination of redundancy, replacement of lacking characteristics, and division. Moreover, it removes unwanted noises in the images.

3.3. Phase 1 Feature Selection and Classification Using L-BOA

3.3.1. Butterfly Optimization Algorithm

The behavior of BOA [4] is similar to that of butterflies when they are looking for food and breeding. The ability of such butterflies to survive for several years is related to their abilities. They use their sense of vision, feel, scent, hearing, and tasting to find a mate and prey. These abilities are in handy when moving from one location to another. The fragrance is the most distinctive of all the organs since it aids the butterflies in seeking nutrition, usually pollen, also at long ranges. The overall procedure of the butterfly is based on two fundamental issues: the construction of Fr and the modification of AS. The letter Fr stands for aroma, and the phrase AS stands for stimulation strength.

The stored optimization problem is connected to the intensity of the actual stimulus AS of the butterflies. On the other hand, the scent Fr is relative and is detected by the surviving butterfly. The odor is considered a function of stimulus intensity in this BOA method, which would be formally expressed in Equation (1).

$$Fr = SmAS^{Pe}. \quad (1)$$

- In the classic BOA method, the terms Sm and Pe are frequently between 0 and 1. Sm represents the perceptual modalities in Equation (1), and the energy exponential depending on modalities is represented by Pe, which indicates the variable absorbing degrees. The qualities of butterflies are glorified in the following areas.
- The optimization problem controls the system increase of the butterflies. The butterfly would be capable of attracting one another due to the fragrance released by all of them.
- Every butterfly would migrate randomly and towards the most incredible butterflies in an attempt to remove the scent.

The beginning process, Iterative process, and Final process” are the three processes of traditional BOA. Every repetition begins with the initial stages, followed by repeated searches, and finally, the method is completed until the best answer is found. The optimal solution and objective function are defined at startup. In addition, the variables which are employed are allocated. Then, for effectiveness, build the butterfly’s

initial solution. The butterfly’s positions are produced randomly in the search process, together with their smell and fitness values, calculated and saved. The total number of butterflies stays constant throughout simulations, and the information is stored in a set system memory.

The traditional BOA method is used to number repetitions throughout the multiple examples. Every cycle computes the fitness values of all the butterflies available in the optimal solution for traveling to new areas. The method calculates the fitness values of the entire butterfly in distinct places initially in the optimal solution. Equation (1) will later generate the smell in these butterflies’ sites. The model’s two main stages are the local and globally searching cycles. The butterflies make a point in the development of the optimization technique, P, and the corresponding formula is Equation (2).

$$LI_i^{-it+1} = LI_i^{-it} + (Rd^2 \times P^* - LI_i^{-it}) \times Fr_i. \quad (2)$$

The answer vectors for the I^{th} butterflies in their repetitions are provided by LI_1^{it} the current best answer from all of the answers in the current round would be provided by p, the random variable among 0 and 1 is provided by Rd, as well as the smell of the I^{th} butterflies is provided by Fr_i in Equation (2). Equation (3) expresses the math problem for the localized search stage. The j^{th} and k^{th} butterfly in repetition is provided by LI_j^{it} and LI_k^{it} , correspondingly, from the optimal s

$$= LI_i^{-it} + (Rd^2 LI_m^{-it}) \times Fr_i \quad (3)$$

Butterflies are seen mating with each other and hunting for nourishment on a national and global level. The switching probability sp is often used in BOA to switch between common international and intense search engines.

3.3.2. Conventional Lion Algorithm

The suggested L-BOA technique for hidden neuron improvement in both NN and DBN. LA [2] gets its main impetus from the environment, where typical lion behaviors include regional conquest and territory protection. The standard LA method has six process steps briefly detailed below.

a Generation of Pride

The territory lions as well as its lioness are referred to as LI^{Ma} and LI^{Fm} , respectively, whereas the migratory

lion is referred to as LI Nom. These wandering lions is not a member of the proud generations. The lion's and lioness's vectors components are provided by LI_{El}^{Ma} , LI_{El}^{Fn} and the word LI_{El}^{Nom} symbolizes the nomadic lion, which are the random numbers amongst bounds if $A < 1$, where $ElNg$. Furthermore, Lng , which would be represented in Equation (4) is used to express the lion's length.

$$Lng = \begin{cases} A; & \text{if } A > 1 \\ B; & \text{Otherwise} \end{cases} \quad (4)$$

The variables A and B in the preceding formula are the numbers used to calculate the lengths of the lions. Whenever a=1 occurs, the method must explore to use of the binary digitized lion, which causes the components of the vector to be constructed as 1 or 0 Equation (5).

$$vlcty(LI_{El}) \in (LI_{El}^{-min}, LI_{El}^{-max}). \quad (5)$$

b Evaluation of Fertility

Following the pride formation process, a reproductive assessment is carried out. The laggard in this case is the lion, and the laggardness ratio is referred to as Lag_{Rt} , which would be increased via one. When $ft(LI^{Ma})$ improves, the standard fitness is referred to as ft_{ref} . The territory defense occurs whenever the laggardness ratio increases Lag_{Rt}^{max} . Furthermore, the lioness' productivity is regulated by the sterilization ratio str_{Rt} , which is increased once when str_{Rt} reaches str_{Rt}^{max} . In this scenario, Equations (6)-(8) are used to modify the lioness.

$$LI_{El}^{Fe+} = \begin{cases} LI_{fl}^{Fe+} & \text{if } El = fl \\ LI_{El}^{Fe} & \text{Otherwise} \end{cases} \quad (6)$$

$$LI_{fl}^{Fe+} = \min[LI_{fl}^{-max}, \max(LI_{fl}^{-min}, \Delta_{fl})] \quad (7)$$

$$\Delta_{fl} = [LI_{fl}^{-Fe} + (0.1 \text{ rnd}_2 - 0.05)(LI_{fl}^{Ma} - \text{rnd}_1 LI_{fl}^{Fe})]. \quad (8)$$

There are two basic phases and one additional phase in this process. The major processes in this process are mutations and crossovers, with gender grouping as a secondary phase.

c Territory Defense

It is a simple approach for exploring the optimum solution, so it aids the method in avoiding the locally optimum solution and locating distinct options with

equal fitness values. Whenever the criteria indicated in Equations (9)-(11) are met, the nomadic lion LI^{Nom} is chosen.

$$ft(LI^{-Nom}) < ft(LI^{-Ma}) \quad (9)$$

$$ft(LI^{-Nom}) < ft(LI^{-mcb}) \quad (10)$$

$$ft(LI^{-Nom}) < ft(Li^{-fcb}). \quad (11)$$

d Ending Process

One of the formulas in Equations (12)-(13) must be achieved for the algorithms to be completed.

$$it > it_{max} \quad (12)$$

$$|ft(LI^{-Ma}) - ft(LI^{-Opt})| \leq err_{thres} \quad (13)$$

In the preceding formulas, the number of iteration is represented by it, which starts at zero and increases by one whenever territory domination is achieved. The error threshold is denoted by the phrase err_{thres} .

3.4. Proposed Lion-based Butterfly Optimization Algorithm (L-BOA)

In previous studies, many optimization methods were combined to create a novel hybrid optimization technique. For certain searching difficulties, these offer the best outcomes. The approach takes into account the benefits of enhancing performance. As comparison to other meta-heuristic algorithms, the hybrid optimization approach appears to have the best convergence behavior [4]. The traditional BOA algorithm is capable of properly tackling the issue. Moreover, that has numerous drawbacks, including convergence rate, a proclivity for local optimization, and reduced performance. The LA method is combined with the BOA algorithm to solve the BOA difficulties, and the result is known as the L-BOA method.

The traditional LA method has had the advantages of becoming exceedingly efficient, having a higher probability of obtaining the globally or adequate optimal solutions, becoming well suited to high-dimensional issues, while being expandable. If $(Rd < sp)$, the updating operation is controlled by Equation (1) in the standard BOA method; alternatively, it is handled by Equation (2). The standard BOA update procedure is used in the suggested L-BOA if the sequence of num-

bers r_d is less than the switching frequency s_p . The female lion, on either hand, performs the updating process using Equation (3).

3.5. Improved YOLO-v4 with CSPDarkNet53

The thickness of the networks develops as the amount of layers of the convolutional neural network increases, and the deeper network structure is useful for extracting object information. As a result, little items' important information is enhanced. The following are the primary YOLO-v4-based enhancements reported in this paper: The CSPDarkNet53 has been enhanced into CSP1 X and CSP2 X, resulting in fewer network modules and lower extracting features variables in the network structure. By using CSP2 X device in Neck can enhance data fusion, as well as the adaptive image scaling model has been used to substitute the image scaling model in YOLO-v4.

3.5.1. Extracting Features in Backbone Network

The residue layer in YOLO-v4 was included to improve the program's learning capacity and decrease the amount of variables. The residual network's operation method and the set of parameters are reduced. The residue component's (Res-unit) function can be summarized in the following points. Execute 1×1 convolution initially, then 3×3 convolution, and finally weighing the component's two outcomes. The goal of weighing is to improve the characteristic layer's data without modifying its information's in the dimension. The picture's collection of element that links is sent into CSPDarkNet53, which then performs continual convolution down-sampling to obtain more contextual features.

Next, in order to obtain more semantic features, continual convolution down-sampling is conducted. As a result, the greatest meaningful information is found during last 3 layers of Backbone, and last three levels of characteristics are chosen as the inputs of SPPNet and PANet. The CSPDarkNet53 network structure is displayed in Figure 2.

Whereas YOLO-v4 employs to define the concept to lower the model's computational energy demands, it still wants to upgrade its memory usage. As a result, the network topology of YOLO-CSPDarkNet53 v4's modules is enhanced in this study to the CSP1 X modules, as seen in Figure 3.

Figure 2

Module structure of CSPDarkNet53

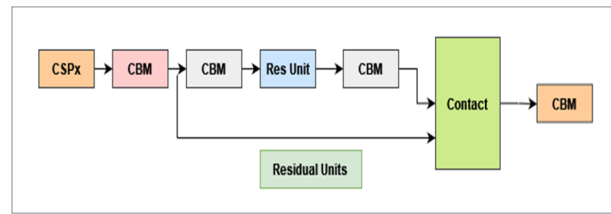
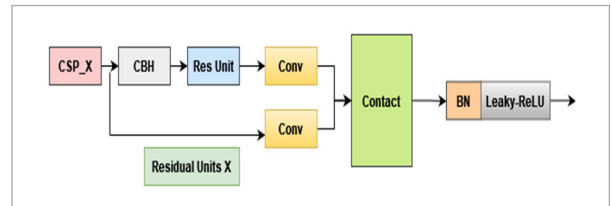


Figure 3

Module Structure of CSP1_X



The enhanced networks, as compared to CSPDarkNet53 in Figure 2, employ the H-swish activation function, given in Equation (14):

$$H - swish(X) = X \frac{ReLU(X+3)}{6}. \quad (14)$$

The computation costs of the Swish function [30], which includes the Sigmoid function, is greater than that of the ReLU method, however the Swish feature is much more efficient than ReLU feature. Howard employed the H-swish feature on portable devices to decrease the model's memory usage, lowering the runtime costs even more. As a result, the benefits of the H-swish functions are exploited in this study to lower the model's operating completion times while assuring there's no gradients inflation, vanishing, or other difficulties. Simultaneously, the model's detection performance has improved.

The original input layers of a residual block in CSP1 X are broken into 2 parts. Again for convolution procedure, the first is being used as the remaining edges. Another is the trunks portion, which executes a 1×1 convolution operation initially, then a 1×1 convolution to modify the channels after reaching the residue blocks, and finally 3×3 convolution operations to improve extraction of features. Finally, the two phases are combined, combining the streams to acquire further data about the set of feature. The enhanced Backbone in this study uses three

CSP1 X modules, while X specifies the amount of residual weighing procedures in the remaining architecture.

Neck Network

The input pictures must be a fixed size for the convolutional neural network to operate. In the previous, the constant inputs for a convolution neural network was acquired via trimming and bending procedures, however these techniques frequently resulted in issues such as item absence or distortion. Authors created SPPNet to solve these issues by removing the ability for a constant input capacity. YOLO-v4 developed the SPPNet structure and management on YOLO-v3 to obtain multi-scale spatial information. They add the CSP2 X modules to the PANet architecture of YOLO-v4 to improve extraction of features and fusion multi-scale local image data with global image data. This enables faster the stream of featured data to improve the accurateness.

In YOLO-v4, the Neck network uses the common convolution technique, but the CSPNet has the benefit of large academic abilities, decreased CPU bottleneck, and limited memory costs. Applying the upgraded CSPNet networking higher unit on YOLO-v4 can increase network convolution layer even more. Such a merged function allows again for top-down transmitting of deeper high - level features in PANet while also fusing the bottom-up deep placement characteristics from of the SPPNet system, allowing for feature engineering among different backbone layer upon layer and recognition layers in the Neck network and much more advanced functions for the Prognostication system.

3.5.2. Adaptive Image Scaling

The picture information provided by the input source inside the high detection rate has a consistent correct size. The writing number identification set of data MNIST, for instance, has a typical image size of 28×28 pixels. ResNet, on the other hand, fixes the input picture to 224×224 because various data collections had various image dimensions. Just at YOLO-v4 detecting network's input source, 2 known dimensions of 416×416 and 608×608 are available. Reducing, bending, extending, resizing, and other traditional procedures for reaching correct size are common, but they can easily result in missing items, a loss of detail, and a drop in correctness.

The picture data had to be manually unified to the

standard size in the earlier convolutional neural network, but YOLO-v4 standardized the size of an image immediately utilizing the information generators and afterwards inputs the picture into the system to accomplish the end-to-end learning experience. The input image sizes in the training and testing phases of YOLO-v4 are 416×416 and 608×608. The actual pictures are sized initially, then grey pictures with sizes of 416×416 or 608×608 are produced, and lastly the scaling picture is layered on the grey image to generate visual information of normal size.

4. Result Analysis

4.1. Simulation Environment

The planned project was carried out on Amazon's cloud. The MATLAB Simulink software, versions 2019a, was used to evaluate the proposed approach. The tests were conducted on a PC with just an Intel Core i7-10700 CPU operating at 2.9 and 4.8 GHz, 8 GB of RAM, and a 64-bit version of Windows 10. The main aim of this analysis was to classify and predict heart disease information, which was crucial in this study. The suggested classifications categorized the information as suggesting the presence of cardiac disease.

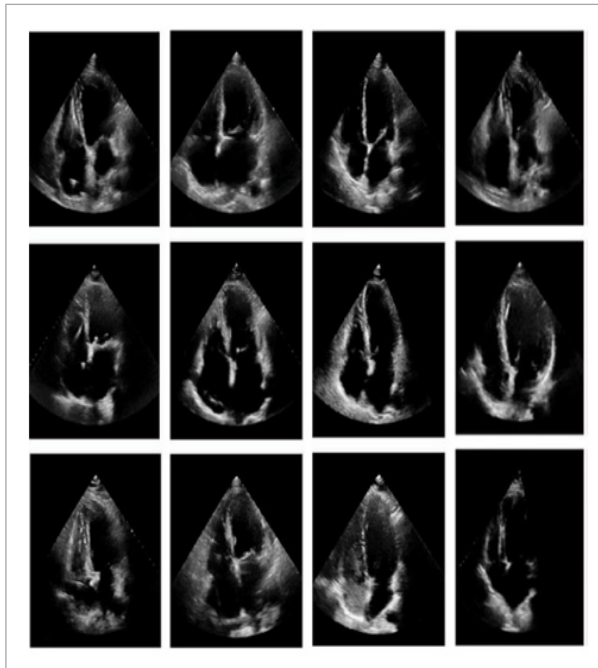
a Descriptions of Dataset

The proposed method was assessed using the Cleveland dataset from the UCI repository, which can be found at <http://archive.ics.uci.edu/ml/datasets.php> (accessed on July 21, 2021). Every set of data has its unique subset of features and qualities; the Cleveland database, for instance, contains 76 features and 303 entries. Just 14 variables from the Cleveland dataset, have been used for training and validation. The suggested model was trained using the whole dataset, and the sensor data acquired was utilized to evaluate the system. All of knowledge was acquired by using sensors, which was used for validation, depending on the characteristics of the training data. In the testing data, the features that were employed in the training examples were also examined.

Figure 4 shows a selection of photos from of the database. The training / testing operations followed this pattern. The photographs from the UCI dataset were utilized for training, while the images captured in real - time basis were used for testing.

Figure 4

Pictures from the dataset as examples



To evaluate the performance of metric measures are using accuracy, specificity, Precision, recall and F-score, values for proposed work LBO-YOLO-v4 is given below.

The LBO-YOLO-v4 method was used to evaluate the experimental assessments of the dataset's healthy and unhealthy type of cases. In the health information categorization, Table 1 shows the accuracy, precision, recall, specificity, and F-score values again for different normal and abnormal classes. Two unique categories of information were reviewed for categorization as normal (healthy) or aberrant in this stage 1 investigation (unhealthy)

Depending on the data, the suggested model was evaluated for accuracy, precision, recalls, specificity, and

F-score. In this evaluation the phase 1, L-BOA method is used it works with Sensor dataset and Cleveland Dataset. The suggested L-BOA method achieved 97.67% accuracy, 96.45% precision, 97.95% recall, 95.40% specificity, and a 96.85% F-score in normal class categorization utilizing smart sensor data received by detectors. Mostly on Cleveland dataset, the L-BOA technique achieved 98.75 % accuracy, 97.85% precision, 98.97% recall, 96.69% specificity, and a 98.79% F-score. The graphic plots for such quality of medical classification process are shown in Figures 5-6.

Figure 5

Phase 1- Normal Classification of Sensor dataset

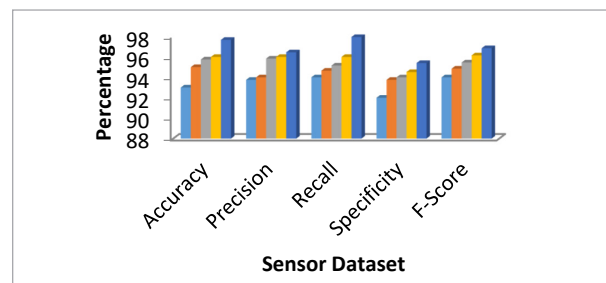


Figure 6

Phase1-Normal Classification of Cleveland dataset

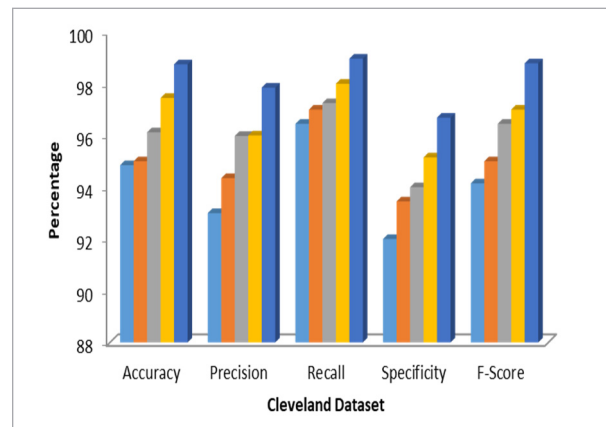


Table 1

Phase 1 output with L-BOA technique was used to compare normal and abnormal class subjects

Dataset	Class Used	Precision	Recall	Accuracy	F-Score	Specificity
Sensor	Abnormal	97.32 %	98.90 %	98.91 %	98.32 %	97.85 %
Cleveland Dataset		96.15 %	98.65 %	98.53 %	97.85 %	97.15 %
Sensor (Collected)	Normal	96.45 %	97.95 %	97.67 %	96.85 %	95.40 %
Cleveland Dataset		97.85 %	98.97 %	98.75 %	98.78 %	96.70 %

The suggested L-BOA method achieved 98.91% accuracy, 97.32% precision, 98.90% recall, 97.85% specificity, and 98.32% F-score in abnormal class categorization using clinical signal data collected by sensors. On the Cleveland d, the L-BOA strategy scored 98.53% accuracy, 96.15% precision, 98.65% recall, 97.15% specificity, and a 97.85% F-score. The graphic plots for such quality of medical classification process for Cleveland dataset are shown in Figures 7-8.

Figure 7

Phase 1-Abnormal Classification of Sensor and Cleveland Dataset

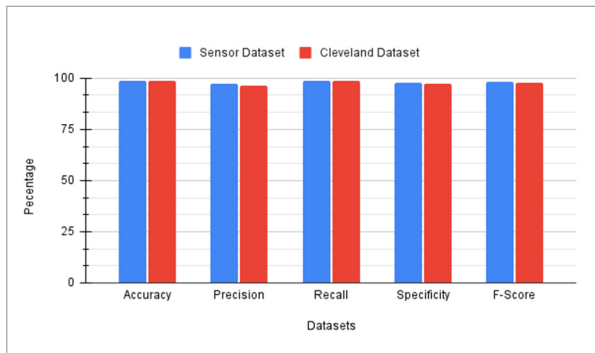
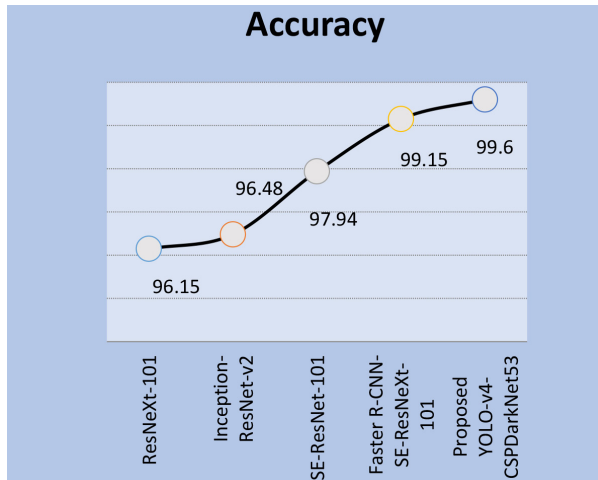


Figure 8

Evaluation of Accuracy



In this evaluation, it works on Phase 2, Improved YOLO-v4 with the CSPDarkNet53 method. Table 2 presents the performance analysis and comparison of the Improved YOLO-v4 with the CSPDarkNet53 medical image classification algorithm with several other existing transfer learning methods. With

Table 2

Output with Phase -2 Comparison of Different algorithms used for image classification

Methods Used	Precision	Recall	Specificity	F-Score
ResNeXt-101	94.00	95.42	92.98	95.99
Inception-ResNet-v2	94.07	96.14	94.11	96.04
SE-ResNet-101	95.18	97.31	95.03	98.25
Faster R-CNN-SE-ResNeXt-101	98.06	98.95	96.32	99.02
Proposed YOLO-v4 with CSPDarkNet53	98.75	99.15	97.05	99.45

98.75% precision, 99.15% recall, 97.05% specificity, a 99.45% F-score, and 99.60% maximum accuracy, the Proposed Improved YOLO-v4 with CSPDarkNet53 outperforms better in other models in all parameters. As demonstrated in Figure 9, the suggested LBO-YOLO-v4 algorithm has greater classification accuracy for classifying echocardiogram images for heart disease prediction.

4.2. Comparison of Phase 1 (L-BOA) and Phase 2 (Improved YOLO-v4 with CSPDarkNet53)

In heart disease prediction both phase 1 and phase 2 is used for classifying and predicting.

While comparing Phase 1 with Phase 2, the Phase 2-(Improved YOLO-v4 with CSPDarkNet53) is improved in all the parameters. In phase-2, it predicts the echocardiogram images. It increases the accuracy level into 1.75%, recall level into 0.18%, precision level into 0.9%, specificity level into 0.35% and F-score

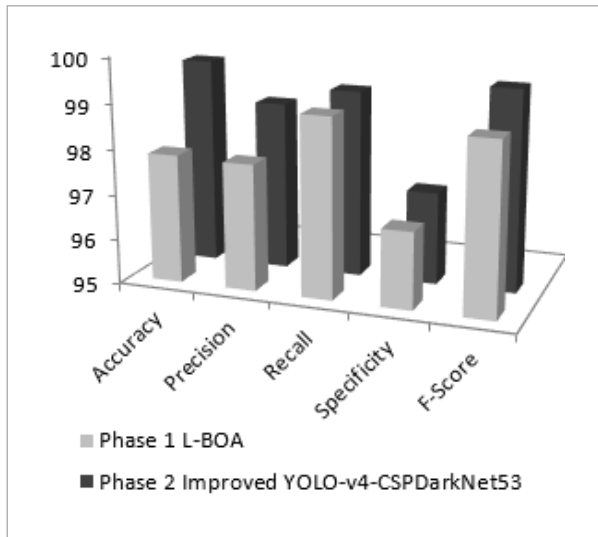
Table 3

Comparison of Phase 1 and Phase 2

Methods Used	Accuracy	Precision	Recall	Specificity	F-Score
Phase 1 (L-BOA)	97.85	97.80	98.9	96.70	98.78
Phase 2 (Improved YOLO-v4 with CSP DarkNet53)	99.60	98.75	99.2	97.05	99.45

Figure 9

Comparisons of Phase 1 and Phase 2



level into 0.67%. In phase 1 it uses IoMT sensor data for predicting the heart disease. It does not give more efficient outcomes. But in phase 2, it uses echocardiogram images for prediction. It gives more efficient outcomes while compared with phase 2. Table 3, shows the comparison of phase 1 and phase 2.

References

- Basheer, S., Alluhaidan, A.S., Bivi, M.A. Real-Time Monitoring Systems for Early Predictions of Heart Diseases Using Internet of Things. *Soft Computing*, 2021, 25, 12145-12158. <https://doi.org/10.1007/s00500-021-05865-4>
- Brisimi, T.S., Xu, T., Wang, T., Dai, W., Adams, W.G., Paschalidis, I. C. Predicting Chronic Disease Hospitalizations from Electronic Health Records: An Interpretable Classification Approach. *Proc. IEEE*, 2018, 106, 690-707. <https://doi.org/10.1109/JPROC.2017.2789319>
- Cabani, A., Hammoudi, K., Benhabiles, H., Melkemi, M. Masked Face-Net-A Dataset of Correctly/Incorrectly Masked Face Images in the Context of COVID-19. *arXiv*, 2020, arXiv:2008.08016. <https://doi.org/10.1016/j.smhl.2020.100144>
- Dubey, A. K. Optimized Hybrid Learning for Multi Disease Prediction Enabled by Lion with Butterfly Optimization Algorithm. *Sadhana*, 2021, 46(2), 1-27. <https://doi.org/10.1007/s12046-021-01574-8>
- Fu, C. Y., Liu, W., Ranga, A., Tyagi, A., Berg, A. DSSD: Deconvolutional Single Shot Detector. *arXiv* 2017, arXiv:1701.06659.
- Haq, A. Q., Li, J. P., Memon, M. H., Khan, J., Malik, A., Ahmad, T., Ali, A., Nazir, S., Ahad, I., Shahid, M. Feature Selection Based on L1-Norm Support Vector Machine and Effective Recognition System for Parkinson's Disease Using Voice Recordings. *IEEE Access*, 2019, 7, 37718-37734. <https://doi.org/10.1109/ACCESS.2019.2906350>
- Hong, W., Xiong, Z., Zheng, N., Weng, Y. A Medical-History-Based Potential Disease Prediction Algorithm. *IEEE Access*, 2019, 7, 131094-131101. <https://doi.org/10.1109/ACCESS.2019.2940644>
- Jeong, J., Park, H., Kwak, N. Enhancement of SSD by Concatenating Feature Maps for Object Detection. *arXiv*, 2017, arXiv:1705.09587. <https://doi.org/10.5244/C.31.76>
- Khan, M. A., Algarni, F. A Health Care Monitoring System for the Diagnosis of Heart Diseases in the IoMT Cloud Environments Using MSSO-ANFIS. *IEEE Access*, 2020, 8, 122259-122269. <https://doi.org/10.1109/ACCESS.2020.3006424>
- Khan, M. A. An IoT Framework for Heart Diseases Predictions Based on MDCNN Classifier. *IEEE Access*,

5. Conclusion

This study presented an IoMT-based cardiac disease prediction model based on machine learning techniques. The developed framework was truly tested twice. Phase 2 is unneeded if the findings of the overall phase are effective and precise in predicting cardiac disease. Medical information received from body of the patient through sensors (wearable's) was utilized for categorization in first phase; echocardiography images have been used for classification in the second phase. Many of these classification systems were used, and the classification methods for prediction of heart disease were confirmed. To identify sensor data, a Hybrid Lion-based Butterfly Optimization Algorithm (L-BOA) approach was applied. For echo image classification, an Improved YOLO-v4 with CSPDarkNet53 model was used. The classifiers are trained using heart disease datasets from the UCI repository, including the Cleveland dataset and the echocardiography dataset. With 98.75% precision, 99.15% recall, 97.05% specificity, a 99.45% F-score, and 99.60% highest accuracy, the proposed scheme Improved YOLO-v4 with CSPDarkNet53 model outperforms conventional models in detecting echocardiography pictures.

- 2020, 8, 34717-34727. <https://doi.org/10.1109/ACCESS.2020.2974687>
11. Karim, A. M., Guzel, M. S., Tolun, M. R., Kaya, H., Celebi, F. V. A New Framework Using Deep Auto-Encoder and Energy Spectral Density for Medical Wave form Data Classification and Processing. *Biocybernetics and Biomedical Engineering*, 2018, 39, 1-12. <https://doi.org/10.1016/j.bbe.2018.11.004>
 12. Li, Z., Zhou, F. FSSD: Feature Fusion Single Shot Multi-box Detector. arXiv 2017, arXiv:1712.00960
 13. Liu, Y., Zhou, H., Tsung, F., Zhang, S. Real-Time Quality Monitoring and Diagnosis for Manufacturing Process Profiles Based on Deep Belief Networks. *Computers and Industrial Engineering*, 2019, 136, 494-503. <https://doi.org/10.1016/j.cie.2019.07.042>
 14. Maqsood, S., Damaševičius, R., Maskeliūnas, R. TTCNN: A Breast Cancer Detection and Classification Towards Computer Aided Diagnosis Using Digital Mammography In Early Stages, *Applied Sciences*, 2022, 12(7), 3273-3300. <https://doi.org/10.3390/app12073273>
 15. Maqsood, S., Damasevicius, R., Shah, F. M., Maskeliūnas, R. Detection of Macula and Recognition of Aged-Related Macular Degeneration In Retinal Fundus Images. *Computing and Informatics*, 2021, 40(5), 957-987. https://doi.org/10.31577/cai_2021_5_957
 16. Manimurugan, S., Almutairi, S., Mohammed Aborokbah, M., Narmatha, C., Ganesan, S., Chilamkurti, N., Riyadh, A., Hani, A. A Two-Stage Classification Model for the Prediction of Heart Disease Using IoMT and Artificial Intelligence. *Sensors*, 2022, 22(2), 476. <https://doi.org/10.3390/s22020476>
 17. Mehmood, A., Iqbal, M., Mehmood, Z., Irtaza, A., Nawaz, M., Nazir, T., Masood, M. Prediction of Heart Diseases Using Deep Convolutional Neural Network. *Arabian Journal for Science and Engineering*, 2021, 46, 3409-3422. <https://doi.org/10.1007/s13369-020-05105-1>
 18. Mohan, S., Thirumalai, C., Srivastava, G. Effective Heart Disease Prediction Using Hybrid Machine Learning Techniques. *IEEE Access*, 2019, 7, 81542-81554. <https://doi.org/10.1109/ACCESS.2019.2923707>
 19. Odusami, M., Maskeliūnas, R., Damaševičius, R. An Intelligent System for Early Recognition of Alzheimer's Disease Using Neuro Imaging, *Sensors*, 2022, 22(3), 740-761. <https://doi.org/10.3390/s22030740>
 20. Pan, Y., Fu, M., Cheng, B., Tao, X., Guo, J. Enhanced Deep Learning Assisted Convolutional Neural Networks for Heart Diseases Predictions on the Internet of Medical Things Platforms. *IEEE Access*, 2020, 8, 189503-189512. <https://doi.org/10.1109/ACCESS.2020.3026214>
 21. Raj, R. J. S., Shobana, S. J., Pustokhina, I. V., Pustokhin, D. A., Gupta, D., Shankar, K. Optimal Features Selections-Based Medical Images Classifications Using Deep Learning Models in Internet of Medical Things. *IEEE Access*, 2020, 8, 58006-58017. <https://doi.org/10.1109/ACCESS.2020.2981337>
 22. Simanta, S. S., An Efficient IoT-Based Patient Monitoring and Heart Diseases Predictions Systems Using Deep Learning Modified Neural Networks. *IEEE Access*, 2020, 8, 135784-135797. <https://doi.org/10.1109/ACCESS.2020.3007561>
 23. Sierra-Sosa, D., Garcia-Zapirain, M. B., Castillo, C., OleagordiaI, Nuno-Solinis, R., Urtaran-Laesgoiti, M., Elmaghraby, A. Scalable Healthcare Assessment for Diabetic Patients using Deep Learning on Multiple GPUs. *IEEE Transaction on Industrial Informatics*, 2019, 15, 5682-5689. <https://doi.org/10.1109/TII.2019.2919168>
 24. Vasquez Morales, G. R., Martinez Monterrubio, S. M., Moreno-Ger, P., Recio-Garcia, J. A. Explainable Prediction of Chronic Renal Disease in the Colombian Population Using Neural Networks and Case-based Reasoning. *IEEE Access*, 2019, 7, 7152900-7152910. <https://doi.org/10.1109/ACCESS.2019.2948430>
 25. Wang, M., Wu, C., Wang, L., Xiang, D., Huang, X. A Feature Selections Approach for Hyperspectral Images Based on Modified Antlion Optimizer. *Knowledge Based System*, 2019, 168, 39-48. <https://doi.org/10.1016/j.knsys.2018.12.031>
 26. Wang, Z.Y., Wang, G., Huang, B., Xiong, Z., Hong, Q., Wu, H., Yi, P., Jiang, K., Wang, N., Pei, Y. Masked Face Recognition Dataset and Application. arXiv 2020, arXiv:2003.09093.
 27. Xiao, Q., Luo, J., Dai, J. Computational Prediction of Human Disease-Associated circRNAs Based on Manifold Regularization Learning Framework. *IEEE Journal of Biomedical Health Informatics*, 2019, 23, 2661-2669. <https://doi.org/10.1109/JBHI.2019.2891779>
 28. Yang, X., Lu, R., Shao, J., Tang, X., Yang, H. An Efficient and Privacy-Preserving Disease Risk Prediction Scheme for E-Healthcare. *IEEE Internet of Things*, 2019, 6, 3284-3297. <https://doi.org/10.1109/JIOT.2018.2882224>
 29. Yu, J., Zhang, W. Face Mask Wearing Detection Algorithm Based on Improved YOLO-v4. *Sensors*, 2021, 21(9), 3263. <https://doi.org/10.3390/s21093263>
 30. Zhang, H., Li, D., Ji, Y., Zhou, H., Wu, W., Liu, K. Toward New Retail: A Benchmark Dataset for Smart Unmanned Vending Machines. *IEEE Transaction on Industrial Informatics*, 2020, 16(12), 7722-7731. <https://doi.org/10.1109/TII.2019.2954956>

